



# The Nonequilibrium Thermodynamics of Atmospheric Blocking

Andrew Jensen<sup>1</sup>

<sup>1</sup>Mathematical Sciences, Northland College, Ashland, 54806, WI, USA

*Correspondence to:* Andrew Jensen (ajensen@northland.edu)

**Abstract.** Two strong NE Pacific blocking events that occurred nearly one year apart and in the same region are examined here by methods from nonequilibrium thermodynamics. In a nonequilibrium setting, the time variation of entropy is a sum of two parts: the external entropy supply and the internal entropy production. The internal entropy production and external entropy supply (the surface entropy supply) are calculated and compared to recent trends in the region that encompassed both blocking events. The entropy production and entropy surface supply were found to be high during both blocking events. However, the surface conditions during the events were markedly different. The surface conditions during the first event were dominated by the NE Pacific sea surface temperature anomaly known as the Blob, while the other event was less influenced. In particular, the surface entropy supply increased from January to February for the first event. The entropy production decreased slightly but any negative entropy flows from extratropical cyclones were offset by the increasing surface entropy supply, maintaining the blocking event. On the other hand, the second event had no large changes in the surface entropy supply or entropy production during its lifetime even though it was similar to the first event in many respects. The use of entropy as a convenient variable to examine the mechanisms that maintain blocking events is considered.

## 1 Introduction

The evolution of blocking anticyclones has been a source of many studies since the pioneering work in Rex (1950a, b). However, despite recent advances, the dynamics of blocking are still not fully understood, Luo et al. (2014), though significant progress has been made. For example, various techniques have been used to investigate the evolution of blocking events, such as low order dynamical models (Charney and Devore, 1979), modons (Haines and Marshall, 1987), and multiscale models (Luo, 2005; Luo et al., 2014), to name a few. The studies employing these techniques, as well as many others, have shed significant light on the dynamics of blocking. However, many studies are purely dynamical and neglect diabatic heating. As shown in Pfahl et al. (2015), diabatic heating plays an important role in blocking events and should be considered in further studies of blocking. To that end, a method of examining atmospheric blocking under the influence of diabatic heating is presented here using techniques from nonequilibrium thermodynamics.

Thermodynamics is usually applied to the atmosphere in an equilibrium setting or under the assumption of local thermodynamic equilibrium, (Zdunkowski and Bott, 2004). However, the atmosphere is a nonequilibrium thermodynamic system, Kleidon (2012). Moreover, irreversible processes in a system lead to positive internal entropy production as a consequence of the second law of thermodynamics, see Zdunkowski and Bott (2004), which in turn lessens the orderliness of the system. On



the other hand, in reversible processes the entropy production vanishes. In a nonequilibrium setting, the time rate of change of entropy can be examined as the sum of two parts: the external entropy supply (flux) and the internal entropy production

$$\frac{dS}{dt} = \frac{dS_{ext}}{dt} + \frac{dS_{int}}{dt}.$$

Expressions for  $\frac{dS_{ext}}{dt}$  and  $\frac{dS_{int}}{dt}$  can be found in (Li et al., 2014; Li and Chylek, 2012) and will be briefly derived below. Now, (Nicolis and Prigogine, 1977; Liu et al., 2004) showed that in order for a system to maintain an orderly state there must be an external supply of low or negative entropy. Otherwise, the orderly structures in a system are dissipated. For example, Liu et al. (2004) examined negative entropy flows in tropical cyclones while Li et al. (2014) examined the negative entropy  
5 advection in extratropical cyclones. However, the application of nonequilibrium thermodynamics to blocking in the manner of Li et al. (2014) has not yet been performed. Indeed, blocking is not expected to exhibit negative entropy flows in the same manner as tropical or extratropical cyclones because of the different dynamics responsible for their genesis, maintenance, and dissipation. In other words, blocking tends to dissipate (block) the orderly structures in a region. Some reasons for using entropy to examine atmospheric processes are the large number of quantities that contribute to the entropy balance, it provides  
10 a means to examine the effects of diabatic heating, and it characterises the dissipative nature of blocking with a single variable in terms of fundamental physics.

In order to apply nonequilibrium thermodynamics to atmospheric blocking events, two complementary Northern Hemisphere blocking events were selected. The two events chosen occurred in nearly the same location and time, but one year apart. Since the events were so similar in spatio-temporal location an analysis of the effects of different surface boundary conditions with  
15 the surface entropy flux and entropy supply on dynamics of the two blocking events can be performed. The first event lasted from Jan 23 - Feb 16, 2014 and was centered at 130° W, while at the same time the anomalously warm sea surface temperatures in the NE Pacific, known as the Blob, were intensifying, (Bond et al., 2015a, b; Jensen, 2015). This association adds another dimension to the present work beyond just the dynamics of blocking since the Blob contributed in a dramatic way to the surface heat fluxes that made up part of the entropy balance. The second event considered here occurred from Jan 28 - Feb 18,  
20 2015 and was centered at 140° W. However, by the time this event formed the positive sea surface temperature anomalies had migrated toward the coast of California and Gulf of Alaska, Bond et al. (2015a, b) and the sensible heat flux in the blocking area was smaller. While the events were similar in many ways, the mechanisms that maintained them can be seen in the entropy calculations below.

The Blob formed under the influence of an anomalously strong ridge in the winter of 2013-2014, see Bond et al. (2015a).  
25 The strong blocking event that formed out of the ridge in early 2014, Jensen (2015), was influenced by diabatic heating (see figure 12 and discussion in Jensen (2015)) as can be seen through the surface entropy supply and entropy production, as will be shown below. The event in early 2015 was also influenced by diabatic heating, as can be seen in the entropy production and surface entropy supply calculations provided below. In particular, the surface entropy supply during both blocking events was much greater than in past years, but especially for the 2015 event during which SST anomalies were highest in the blocking  
30 region.



The importance of this work is severalfold. Nonequilibrium thermodynamics as used here has not yet been applied to blocking. The causes and consequences of both blocking events under consideration here are important to examine because of their role in the maintenance of California's drought. The surface supply of entropy from the Blob has not been examined and is shown to be large compared to the surface entropy supply in the same location during previous years. The role of heat fluxes in blocking events is also examined by means of the surface entropy supply. Furthermore, the entropy production and surface entropy supply provide an alternate perspective of the mechanisms that sustain blocking events and the manner in which they interact with their surroundings. Below, the entropy balance equation is derived with the entropy production and surface entropy supply. The results of calculations are presented. Next, a discussion of the results is provided and conclusions are drawn.

## 2 Entropy Production and Surface Entropy Supply

As described in (Emanuel, 1994; Li et al., 2014; Li and Chylek, 2012), the balance equation for the specific entropy  $s$  is

$$s = c_{pd} \ln \theta + \frac{\lambda q_v}{T} - R_v q_v \ln H. \quad (1)$$

The symbols  $c_{pd}$ ,  $T$ ,  $\theta$ ,  $q_v$ ,  $\lambda$ ,  $R_v$ ,  $H$  are the specific heat at constant pressure for dry air, temperature, potential temperature, specific humidity, latent heat of vaporization, gas constant for water vapor, and the relative humidity, respectively. In this section we follow the development of the entropy balance equation in (Li and Chylek, 2012; Li et al., 2014). Differentiation of

(1) yields

$$\frac{ds}{dt} = \frac{c_{pd}}{\theta} \frac{d\theta}{dt} + \frac{\lambda}{T} \frac{dq_v}{dt} - R_v \ln(H) \frac{dq_v}{dt}. \quad (2)$$

As explained in Li and Chylek (2012),  $\frac{d \ln H}{dt}$  and terms with  $\frac{1}{T^2}$  may be neglected since they are two orders of magnitude smaller than the other terms in the equation. Now, using the first law of thermodynamics and the balance equation for specific humidity, a form of the entropy equation amenable to computation can be derived.

To that end, the first law of thermodynamics can be written (Li and Chylek, 2012) as

$$\frac{T}{\theta} \frac{d\theta}{dt} = Q_r + Q_h + Q_f + Q_1 + \frac{\lambda}{c_{pd}} (C - E). \quad (3)$$

The symbols  $Q_r$ ,  $Q_h$ ,  $Q_f$ ,  $Q_1$  are the diabatic heating rates corresponding to radiation, sensible heating, frictional heating, and deep/shallow convection, respectively.  $C$  and  $E$  are the condensation and evaporation rates. In flux form (3) becomes

$$\frac{T}{\theta} \frac{d\theta}{dt} = -\frac{1}{c_{pd}\rho} \left( \frac{\partial F_h}{\partial z} - \rho \tau_{3,\alpha} \frac{\partial u_\alpha}{\partial z} \right) + Q_1 + \frac{\lambda}{c_{pd}} (C - E) + Q_r, \quad (4)$$

with the Einstein summation convention on the indices  $\alpha = 1, 2, 3$ .  $F_h$ , is the sensible heat flux and  $\tau$  is the surface wind stress.

Now, the balance equation for  $q_v$  can be written as

$$\frac{dq_v}{dt} = \frac{c_{pd} Q_l}{\lambda} - \frac{c_{pd} Q_2}{\lambda} + E - C = -\frac{1}{\lambda \rho} \frac{\partial F_l}{\partial z} - \frac{c_{pd} Q_2}{\lambda} + E - C. \quad (5)$$

The symbols  $Q_l$ ,  $F_l$ ,  $Q_2$  represent the latent heat due to vertical turbulent diffusion, the corresponding latent heat flux, the moistening heating in deep/shallow convection, respectively.



By using the equation of continuity and equations (2), (3), (4), and (5), the final form of the entropy balance equation is

$$\frac{\partial \rho s}{\partial t} + \frac{\partial \rho u_i s}{\partial x_i} = - \frac{\partial}{\partial z} \left( \frac{F_h + F_l + F_c}{T} - \frac{\rho u_\alpha \tau_{3,\alpha}}{T} - R_v \frac{F_l - F_{cm}}{\lambda} \ln H \right) + \sigma + c_{pd} \rho \frac{Q_r}{T} \quad (6)$$

where  $\sigma$  is the internal entropy production

$$\sigma = (F_h + F_l + F_c) \frac{\partial}{\partial z} \frac{1}{T} - \rho u_\alpha \frac{\partial}{\partial z} \frac{\tau_{3,\alpha}}{T} - R_v \frac{F_l + F_{cm}}{\lambda} \frac{\partial \ln H}{\partial z} + R_v \rho (C - E) \ln H \quad (7)$$

5 The surface entropy supply (external entropy supply) is given by

$$\Sigma = \left( \frac{F_h + F_l}{T} - \frac{\rho u_\alpha \tau_{3,\alpha}}{T} - R_v \frac{F_l}{\lambda} \ln H \right) \Big|_{z=0}. \quad (8)$$

### 3 Methods

The entropy production (equation (7)) and surface entropy supply (equation (8)) were calculated for the region 180° W to 100° W and 35° N to 75° N in order to encompass both of the blocking events examined here, as well as the anomalously high sea surface temperatures in the NE Pacific Ocean during the Winter of 2013-2014. The entropy production was vertically integrated as in Li et al. (2014) from the surface to 250 hPa. The NASA MERRA reanalysis (Rienecker et al., 2011) data set with a horizontal resolution of 2/3° longitude by 1/2° latitude was used to compute the entropy production and surface entropy supply. The blocking events were identified using the methodology found in (Lupo and Smith, 1995; Wiedenmann et al., 2002) and used in various other references, (see e.g., Mokhov et al., 2014; Jensen, 2015).

In order to quantify the strength of each blocking event, following Wiedenmann et al. (2002), the dimensionless quantity can be defined:

$$\text{BI} = 100 \left[ \left( \frac{Z_{max}}{Z} \right) - 1 \right].$$

15 This quantity is a measure of the blocking event intensity; it provides a measure of the amplitude of the quasi-stationary wave in the blocking region.  $Z_{max}$  is the maximum 500 hPa height in the closed anticyclone region while  $Z$  is the 500 hPa height contour encompassing the upstream and downstream troughs.

### 4 Description of the Two Events

In this section a brief description of both blocking events is given, including their similarities and differences. Figures 1 and 2 demonstrate how similarly placed spatially the two blocking events considered in this study were.

Event 1: Following Jensen (2015), the first event was a long-lived large amplitude event with an average BI of 5.93, which indicates that the event was strong, Wiedenmann et al. (2002). It lasted from Jan 23-Feb 16, 2014 and was centered at 130° W, (see Figure 1), although the event migrated westward during its life cycle. This event formed out of the strong drought-associated ridge over the West Coast of the US during winter 2013-2014. The blocking event survived an abrupt change in the planetary-scale flow when the Pacific North America (PNA) pattern index changed from positive to negative in early February.



In addition, positive SST anomalies were as high as 4° C in the region during early February. As noted in the Introduction, these anomalies were a response in part to the strong ridging in the region prior to the blocking event. As described in (Jensen, 2015; Bond et al., 2015a), anomalous sea surface temperatures changed during the early part of February coinciding nearly with the reintensification of the blocking event after a precipitous decline in the BI, Jensen (2015). This suggests that the sea surface temperature anomalies and the blocking event were coupled, as can be seen in the surface entropy flux calculations below. Jensen (2015) concluded that the event survived the change in planetary-scale flow because of fluxes of negative potential vorticity. In the context of this study, the surface entropy supply contributed positive entropy to the region when its entropy production was dropping (during the decline in BI) to maintain the event, as can be seen in the Results section.

Event 2: The second event (see Figure 2) was also long-lived and large amplitude with an average BI of 4.19. It lasted from Jan 28-Feb 18, 2015 and was centered at 140° W. However, a significant difference between this event and the other described previously was that there was no dramatic change in the planetary-scale flow pattern during this event, in contradistinction to the 2014 event (see <http://www.ncdc.noaa.gov/sotc/synoptic/201501>). Another significant difference between the two events was the influence of the Blob on the surface boundary conditions. By the time this event formed, the positive SST anomalies associated with the Blob had migrated toward the coast of California and the Gulf of Alaska, see (Bond et al., 2015a, b). Since the surface conditions and large-scale dynamics were different, the effects of different surface boundary conditions on the maintenance of the events was examined using the surface entropy supply and entropy production.

## 5 Results

The results of the calculations of vertically integrated entropy production and surface entropy supply can be found in the Tables. In order to put the results in perspective, the average and variance of both entropy production and surface entropy supply were calculated for the region 180° W to 100° W and 35° N to 75° N during 2010-2012, see Table 3. This period was selected to provide a touchstone for comparing the results obtained for the two blocking events, not a full climatology. For a more extensive climatology, see Li and Chylek (2012). The average entropy production in the region during 2010-2012 was found to be 0.10 and the average surface entropy supply in the region was found to be 0.03. The variances for entropy production and surface entropy supply were 0.01 and 0.02, respectively. As an approximate confirmation of these results, in Figure 3 of Li and Chylek (2012) the 10-year Northern Hemisphere DJF surface entropy flux at the approximate location of the events here can be seen to be approximately 0.10. The average and variance suggest that both the entropy production and surface entropy flux were anomalously high during both of the blocking events, see Tables 1 and 2.

As seen in Table 1, the entropy production during January 2014 was higher than the 2010-2012 average, while the surface entropy supply was an order of magnitude higher than the recent average value in the region. In February 2014, the entropy production dropped slightly reflecting the changes in the large-scale dynamics discussed previously, but still remained above recent trends in the region. The surface entropy supply increased as the sea surface temperature anomaly in the region strengthened because of large sensible heat fluxes. The small variance, see Table 3, suggests that the values of entropy production and surface entropy supply were anomalously high throughout the event. Further, using a rough calculation from the reanalysis



output, the average magnitude of the Bowen ratio in the region during the blocking event was 7.46. The high number indicates the importance of sensible heating for the maintenance of this event as the largest contributor to the surface entropy supply.

In January 2015 (see Table 2) the entropy production and surface entropy supply were also higher than the 2010-2012 average. The variance was small for both variables (Table 3), suggesting that the entropy production and surface entropy supply were anomalously high during the blocking event. In February 2015 there was very little difference in the entropy production from January, and no change in the surface entropy supply. The average magnitude of the Bowen ratio in the region during the 2015 blocking event was 0.23. This number indicates that the importance of sensible heating for maintenance of this blocking event was far less than the 2014 one. Overall, for this event, the entropy production and surface entropy supply were still high, but not by as much as the 2014 blocking event. Most notably, the surface entropy supply was higher in the 2014 event, reflecting the influence of the Blob. In particular, the sensible heat flux accounts for the higher surface entropy supply in 2014 compared to 2015.

## 6 Discussion

As seen in Tables 1 and 2 there was more variation in the entropy production and surface entropy supply between January 2014 and February 2014, than in the 2015 event. This was likely due to the strengthening of the sea surface temperature anomalies in early February 2014. The variation in the entropy variables also occurred during a change in planetary-scale regime, as discussed in detail in Jensen (2015). This change in the large-scale flow also likely had an influence on the change in the entropy variables from January to February 2014. The variation in surface entropy supply reflects the different surface conditions prevailing during the two events under consideration here.

As explained in Jensen (2015), the 2014 event likely would not have survived the planetary-scale regime transition had it not been for eddy fluxes of potential vorticity. From another perspective, the influence of the SST anomalies as reflected in the surface entropy supply calculations here, likely had a role in maintaining the blocking event against demise by the change in large-scale dynamics in the following way. The blocking state was in part maintained by adding large amounts of entropy to the atmosphere when the entropy production was decreasing, the exact opposite of the negative entropy flows in highly organized phenomena such as tropical or extratropical cyclones, (see Liu et al. (2004); Li et al. (2014)). In addition, the BI may be calculated as a daily quantity. The peak BI for the 2014 event was during early February at the same time as the sea surface temperature anomalies in the region reached their most extreme values, (see Bond et al. (2015a) and Figure 3 in Jensen (2015)). This occurred as the surface entropy supply increased from January to February in 2014. On the other hand, the 2015 event had no large changes in the surface entropy supply or entropy production during its lifetime, reflecting the less erratic nature of the surface conditions and large-scale dynamics as well.



## 7 Conclusions

Starting from the entropy balance equation, the entropy production and surface entropy supply have been calculated for two similar blocking events. These two blocking events were similar in many ways: their longevity, amplitudes, and spatio-temporal location. One of the events was dominated by the influence of strong SST anomalies, while the other was less so. The SST anomalies during the 2014 blocking event analyzed here influenced the maintenance of the event through increasing surface entropy flux from January to February 2014. This can be seen in the surface entropy supply calculations in Table 1. The surface conditions did not vary appreciably in the 2015 event, as can be seen in the calculations of surface entropy supply (Table 2). Thus, the anomalous surface conditions had a profound effect on the longevity of the 2014 event and less so for the 2015 event in the following way. As already described, the 2014 event was not expected to endure given the changes in the large-scale dynamics. The flux of entropy into the region may have had a role in maintaining the event against demise. No such changes occurred in the 2015 event. However, the disparity in surface conditions and large-scale dynamics led to similar blocking statistics. Indeed, the entropy calculations here, are another means to examine the mechanisms that maintained the blocking events in this study and in general. Specifically, the largeness of the surface entropy flux and entropy production during the blocking indicate that coherent phenomena in the blocking region were dissipated.

Entropy production and surface entropy supply provide another perspective from which to examine the influence of heating on blocking events. In particular, in this study, the sensible heat flux was the largest contributor to the surface entropy supply and the entropy production in both events. However, less so for the 2015 event as evidenced by the lower Bowen ratio in the region during that event compared to 2014, (see Results). This complements recent work in Pfahl et al. (2015) showing that latent heat release from clouds affects blocking. The surface entropy supply (dominated by sensible heat flux) was large for the 2014 event, which was characterized by significant sea surface temperature anomalies. The surface entropy supply was large relative to past years for the 2015 event also, though less can be concluded other than that the large surface supply of entropy maintained the event. Thus, the surface entropy supply provides alternative means to investigate further the role of sensible heating during blocking.

The primary limitation of this method is the uncertainty in the flux variables in reanalysis and climate models. However, this study affirms that the role of sensible heat should be assessed in studies of blocking, as it may have a significant effect, as in the 2014 event considered here. This study also confirms the usefulness of the techniques from nonequilibrium thermodynamics in blocking, as well as extratropical cyclones, etc., as in Li et al. (2014). Future studies will examine entropy flows from extratropical cyclones during the genesis and destruction of blocking events.

*Acknowledgements.* The author would like to thank NASA MERRA project website for providing the data used in this study as well as Northland College for providing the space and resources to work on this manuscript.



## References

- Bond, N.A., Cronin, M.F., Freeland, H., and Mantua, N.: Causes and impacts of the 2014 warm anomaly in the NE Pacific, *Geophys. Res. Lett.*, 42, 3414-3420, DOI: 10.1002/2015GL063306, 2015.
- Bond, N.A., Cronin, M.F., and Freeland, H.: The Blob: an extreme warm anomaly in the Northeast Pacific [in "State of the Climate in 2014"], *Bull. Amer. Meteor. Soc.*, 96(7), S62 - S63, 2015
- Charney, J.G. and Devore, J.G.: Multiple flow equilibria in the atmosphere and blocking, *J. Atmos. Sci.*, 36, 1205 - 1216, 1979.
- Emanuel, K.A.: *Atmospheric Convection*, Oxford University Press: Oxford, 1994.
- Haines, K. and Marshall, J.: Eddy-forced coherent structures as a prototype of atmospheric blocking, *Q.J.R. Meteorol. Soc.*, 113, 681-704, 1987.
- Jensen, A.D.: A dynamic analysis of a record breaking winter season blocking event, *Adv. Met.*, Article ID 634896, 2015.
- Kleidon, A.: How does the Earth system generate and maintain disequilibrium and what does it imply for the future of the planet?, *Phil. Trans. R. Soc. A*, 270, 1012 - 1040, 2012.
- Li, J., Chylek, P., and Zhang, F.: The dissipation structure of extratropical cyclones, *J. Atmos. Sci.*, 71, 69 - 88, 2014.
- Li, J., Chylek, P.: Atmospheric entropy. Part I: Climate dissipation structure, *J. Clim.*, 25, 3173 - 3190, 2012.
- Liu, C., and Liu, Y.: Negative entropy flow and its effect on the organization of synoptic-scale severe atmospheric systems, *Geophys. Res. Lett.*, 31, L01108, DOI:10.1029/2003GL018071, 2004.
- Luo, D.: A barotropic envelope rossby soliton model for block-eddy interaction. Part I: Effect of topography, *J. Atmos. Sci.*, 62, 5 - 21, 2005.
- Luo, D., Cha, J., Zhong, L., and Dai, A.: A nonlinear interaction model for atmospheric blocking: The eddy-blocking matching mechanism, *Q.J.R. Meteorol. Soc.*, DOI:10.1002/qj.2337, 2014.
- Lupo, A.R. and Smith, P.J.: Climatological features of blocking anticyclones in the Northern Hemisphere, *Tellus*, 47A, 439-456, 1995.
- Mokhov, I.I., Timazhev, A.V., and Lupo, A.R.: Changes in the atmospheric blocking characteristics within Euro-Atlantic region and Northern Hemisphere as a whole in the 21st century from model simulations using RCP anthropogenic scenarios, *Glob. Planet. Chan.*, 122, 265 - 270, 2014.
- Nicolis, G. and Prigogine, I.: *Self-organization in Non-equilibrium systems*, John Wiley & Sons Inc, New York, 1977.
- Pfahl, S., Schwierz, C., Croc-Maspoli, M., Grams, C.M., and Wernli, H.: Importance of latent heat release in ascending air streams for atmospheric blocking, *Nature Geosci.*, 8, 610 - 614, 2015.
- Rex, D.F.: Blocking action in the middle troposphere and its effect on regional climate I: The Climatology of blocking action, *Tellus*, 2, 196-211, 1950a.
- Rex, D.F.: Blocking action in the middle troposphere and its effect on regional climate II: The Climatology of blocking action, *Tellus*, 3, 275-301, 1950b.
- Reinecker, M.M. and Coauthors: MERRA: NASA's modern-era retrospective analysis for research and applications. *J. Clim.* 24 : 3624-3648, 2011.
- Wiedenmann, J.M., Lupo, A.R., Mokhov, I.I., and Tikhonova, E.: The climatology of blocking anticyclones for the Northern and Southern Hemisphere: Block Intensity as a diagnostic, *J. Clim.*, 15, 3459-3473, 2002.
- Zdunkowski, W. and Bott, A.: *Thermodynamics of the Atmosphere*, Cambridge University Press: Cambridge, 2014.



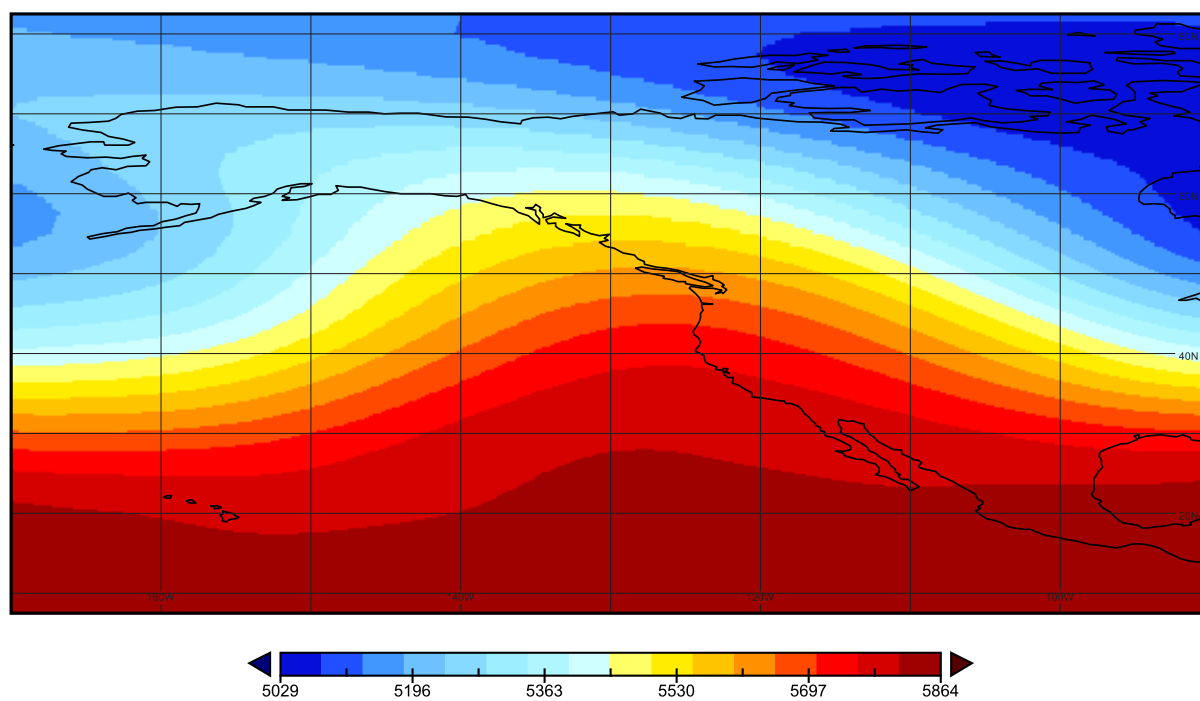


**Figure 1.** Average 500 hPa geopotential heights for January-February 2014.

**Table 1.** Results of the calculations of entropy production and surface entropy supply during Jan-Feb 2014 in  $\text{Wm}^{-2}\text{K}^{-1}$ .

Month	Entropy Production	Surface Entropy Flux
Jan 2014	0.18	0.22
Feb 2014	0.15	0.26
Total	0.33	0.48
Average	0.165	0.24

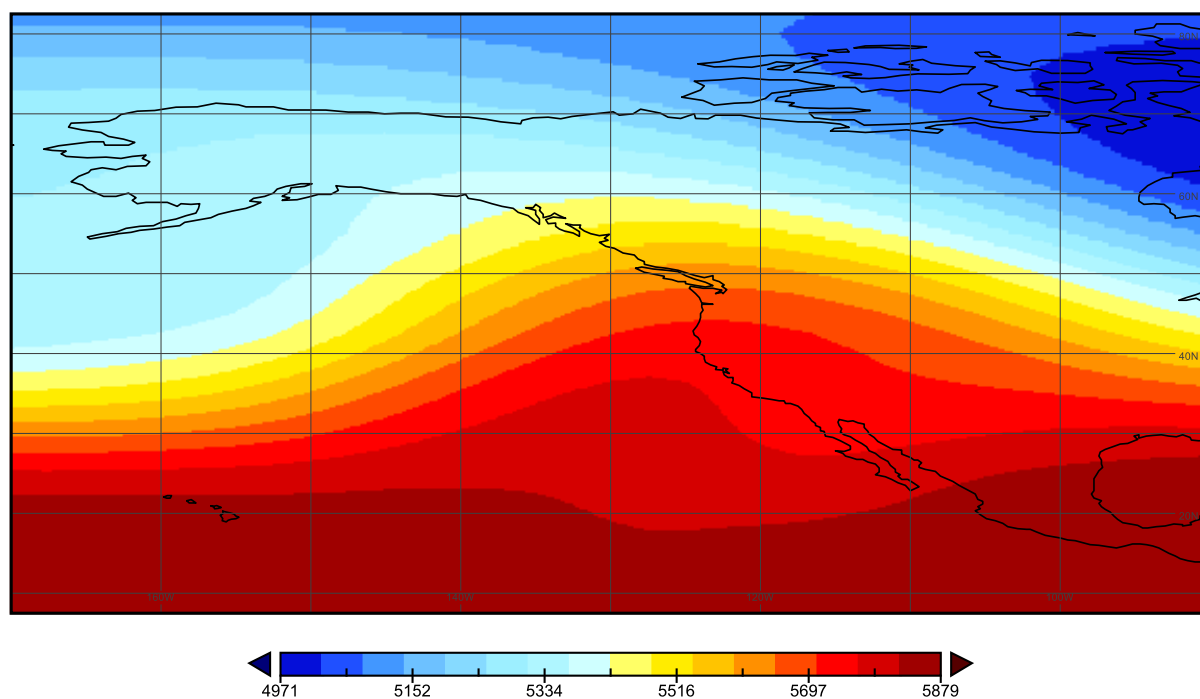


**Figure 2.** Average 500 hPa geopotential heights for January-February 2015.

**Table 2.** Results of the calculations of entropy production and surface entropy supply during Jan-Feb 2015 in  $\text{Wm}^{-2}\text{K}^{-1}$ .

Month	Entropy Production	Surface Entropy Flux
Jan 2015	0.15	0.17
Feb 2015	0.14	0.17
Total	0.29	0.34
Average	0.145	0.17



**Table 3.** Average and variance for 2010-2012 in the blocking region in  $\text{Wm}^{-2}\text{K}^{-1}$ .

Variable	Average	Variance
Entropy Production	0.1	0.01
Surface Entropy Supply	0.03	0.02